CAMS Service Evolution

D1.3 Report on the selection of suitable sensors and channels

Due date of deliverable	June 2024
Submission date	5th July 2024
File Name	CAMEO-D1-3-V1.1
Work Package /Task	WP1 T1.1.3
Organisation Responsible of Deliverable	BSC
Author name(s)	Jeronimo Escribano, Emanuele Emili
Revision number	V1.1
Status	Issued
Dissemination Level	Public

Funded by the European Union

The CAMEO project (grant agreement No 101082125) is funded by the European Union.
Views and opinions expressed are however those of the author(s) only and do not necessarily reflect those of the European Union or the Commission. Neither the European Union nor the granting authority can be held responsible for them.

1 Executive Summary

Copernicus Atmosphere Monitoring Service (CAMS) aerosol analysis and forecasts currently relies on the assimilation of aerosol optical depth (AOD), which are retrieved from short-wave radiance measurement on board satellites. Work Package 1 of CAMS Evolution (CAMEO) will implement a functional prototype of visible radiance assimilation in the operations CAMS service. The direct assimilation of radiances in the IFS allows the best use of the information captured by the satellites, while maintaining the consistency in the assimilation procedure, IFS cloud and aerosols models and simulated fields. In a successful and proved future implementation, the assimilation of short-wave radiances can also be used in long-term aerosols reanalyses, looking back and forward in time from the actual AOD satellite products.

The implementation of visible radiance assimilation in WP1 is being done in the same framework as the numerical weather prediction radiance assimilation in the IFS for longer wavelengths. Visible radiances are sensitive to the surface properties, clouds and aerosols. Therefore, the ingestion of this information in the assimilation can potentially help constraining aerosols and clouds in the IFS. In addition, and because of constraints on computational cost, the assimilated observations for this prototype are expected to be limited to one or, at most, two channels of the same satellite instrument.

This deliverable uses a 1D-Var system to show insights and recommendations on the channel and control vector selection suitable for a first implementation of the short-wave radiance assimilation system. Accordingly, we have designed and performed a set of synthetic experiments where these variables can be evaluated, by considering a plausible set of viewing geometries, aerosol and clouds vertical profiles and load. This report shows that the assimilation of one or two visible channel could have a clear positive impact for some combinations of clouds and aerosols burdens, being the two-channel assimilation more useful in complex cases. The joint estimation of both cloud and aerosol variables improves scores with respect to the prior only when using two channels of the satellite instrument.

Table of Contents

1 Executive Summary 2
2 Introduction 4
2.1 Background 4
2.2 Scope of this deliverable 4
2.2.1 Objectives of this deliverables 4
2.2.2 Work performed in this deliverable 4
2.2.3 Deviations and counter measures 4
2.2.4 CAMEO Project Partners: 5
3 Method and description of the numerical experiments 6
3.1 Control vector 7
3.2 Observations 8
3.3 Scores and subset of experiments 10
4 Results 11
4.1 Only COD in the control vector 13
4.1.1 Atmosphere with clouds, no aerosols 13
4.1.2 Atmosphere with aerosols over clouds 14
4.1.3 Atmosphere with clouds over aerosols 15
4.2 Only AOD in the control vector 17
4.2.1 Atmosphere with aerosols, no clouds 17
4.2.2 Atmosphere with aerosols over clouds 17
4.2.3 Atmosphere with clouds over aerosols 18
4.3 Joint control of AOD and COD 20
4.3.1 Atmosphere with aerosols over clouds 20
4.3.2 Atmosphere with clouds over aerosols 21
4.4 Summary of scores 21
5 Conclusion 25
6 Appendix 1: Summary plots for other configurations 26
6.1 RTM truth: DISORT, observation operator: FLOTSAM, 0.000001% obs. error 26
6.2 RTM truth: FLOTSAM, observation operator: FLOTSAM, 1% obs. error 27
6.3 RTM truth: FLOTSAM, observation operator: FLOTSAM, 0.000001% obs. error 29
7 Appendix 2: Comparison of RTMs reflectances 32

2 Introduction

2.1 Background

Monitoring the composition of the atmosphere is a key objective of the European Union's flagship Space programme Copernicus, with the Copernicus Atmosphere Monitoring Service (CAMS) providing free and continuous data and information on atmospheric composition.

The CAMS Service Evolution (CAMEO) project will enhance the quality and efficiency of the CAMS service and help CAMS to better respond to policy needs such as air pollution and greenhouse gases monitoring, the fulfilment of sustainable development goals, and sustainable and clean energy.

CAMEO will help prepare CAMS for the uptake of forthcoming satellite data, including Sentinel-4, -5 and 3MI, and advance the aerosol and trace gas data assimilation methods and inversion capacity of the global and regional CAMS production systems.

CAMEO will develop methods to provide uncertainty information about CAMS products, in particular for emissions, policy, solar radiation and deposition products in response to prominent requests from current CAMS users.

CAMEO will contribute to the medium- to long-term evolution of the CAMS production systems and products.

The transfer of developments from CAMEO into subsequent improvements of CAMS operational service elements is a main driver for the project and is the main pathway to impact for CAMEO.

The CAMEO consortium, led by ECMWF, the entity entrusted to operate CAMS, includes several CAMS partners thus allowing CAMEO developments to be carried out directly within the CAMS production systems and facilitating the transition of CAMEO results to future upgrades of the CAMS service.

This will maximise the impact and outcomes of CAMEO as it can make full use of the existing CAMS infrastructure for data sharing, data delivery and communication, thus supporting policymakers, business and citizens with enhanced atmospheric environmental information.

2.2 Scope of this deliverable

2.2.1 Objectives of this deliverables

This project will implement the assimilation of calibrated radiances in IFS. Aerosols will be included in the control vector, but the information can be also beneficial for cloud variables. Due to operational constraints, the first implementation of this system can assimilate only one or two channels of visible radiances in the system. Therefore, this report aims to inform into the possibility of including variables related to clouds in the control vector, as well as the impact of using one or two short-wave channels in the assimilation.

2.2.2 Work performed in this deliverable

In this deliverable the work as planned in the Description of Action (DoA, WP1 T1.1.3) was performed.

2.2.3 Deviations and counter measures

No deviations have been encountered.

2.2.4 CAMEO Project Partners:

ECMWF	EUROPEAN CENTRE FOR MEDIUM-RANGE WEATHER FORECASTS
Met Norway	METEOROLOGISK INSTITUTT
BSC	BARCELONA SUPERCOMPUTING CENTER-CENTRO NACIONAL DE SUPERCOMPUTACION
KNMI	KONINKLIJK NEDERLANDS METEOROLOGISCH INSTITUUT-KNMi
SMHI	SVERIGES METEOROLOGISKA OCH HYDROLOGISKA INSTITUT
BIRA-IASB	INSTITUT ROYAL D'AERONOMIE SPATIALEDE BELGIQUE
HYGEOS	HYGEOS SARL
FMI	ILMATIETEEN LAITOS
DLR	DEUTSCHES ZENTRUM FUR LUFT - UND RAUMFAHRT EV
ARMINES	ASSOCIATION POUR LA RECHERCHE ET LE DEVELOPPEMENT DES METHODES ET PROCESSUS INDUSTRIELS
CNRS	CENTRE NATIONAL DE LA RECHERCHE SCIENTIFIQUE CNRS
GRASP-SAS	GENERALIZED RETRIEVAL OF ATMOSPHERE AND SURFACE PROPERTIES EN ABREGE GRASP
CU	UNIVERZITA KARLOVA
CEA	COMMISSARIAT A L ENERGIE ATOMIQUE ET AUX ENERGIES ALTERNATIVES
MF	METEO-FRANCE
TNO	NEDERLANDSE ORGANISATIE VOOR TOEGEPAST NATUURWETENSCHAPPELIJK ONDERZOEK TNO
INERIS	INSTITUT NATIONAL DE L ENVIRONNEMENT INDUSTRIEL ET DES RISQUES - INERIS
IOS-PIB	INSTYTUT OCHRONY SRODOWISKA - PANSTWOWY INSTYTUT BADAWCZY
FZJ	FORSCHUNGSZENTRUM JULICH GMBH
AU	AARHUS UNIVERSITET
ENEA	AGENZIA NAZIONALE PER LE NUOVE TECNOLOGIE, L'ENERGIA E LO SVILUPPO ECONOMICO SOSTENIBILE

3 Method and description of the numerical experiments

Tests are performed by means of 1D-Var software developed in previous CAMS_43 contracts and reported in the following documents: CAMS43_2018SC3_D43.3.4.1_20190331_1Dvar, CAMS43_2019SC1_D3.1.1_201912_FLOTSAM, CAMS43_2021SC2_D3.3.1_202106_SatelliteAssim, CAMS43_2021SC2_D3.3.2_202108_SatelliteAssimLand.

The observation operator of this system is simulating observations for aerosol short-wave radiance assimilation, and it can handle controls over the AOD per aerosol type or total, the profile of the AOD, the surface reflectance (in a limited way), or parameters regarding the aerosol type definitions (complex refractive index, particle size distribution, etc.). For this report, it has been extended to allow computations with clouds in the state and control vectors. Here, we have implemented cloud types of OPAC (and their modified gamma size distribution), along with the existing implementation of OPAC aerosol types. Figure 1 shows the size distributions implemented in the 1D-Var for synthetic observation experiments.

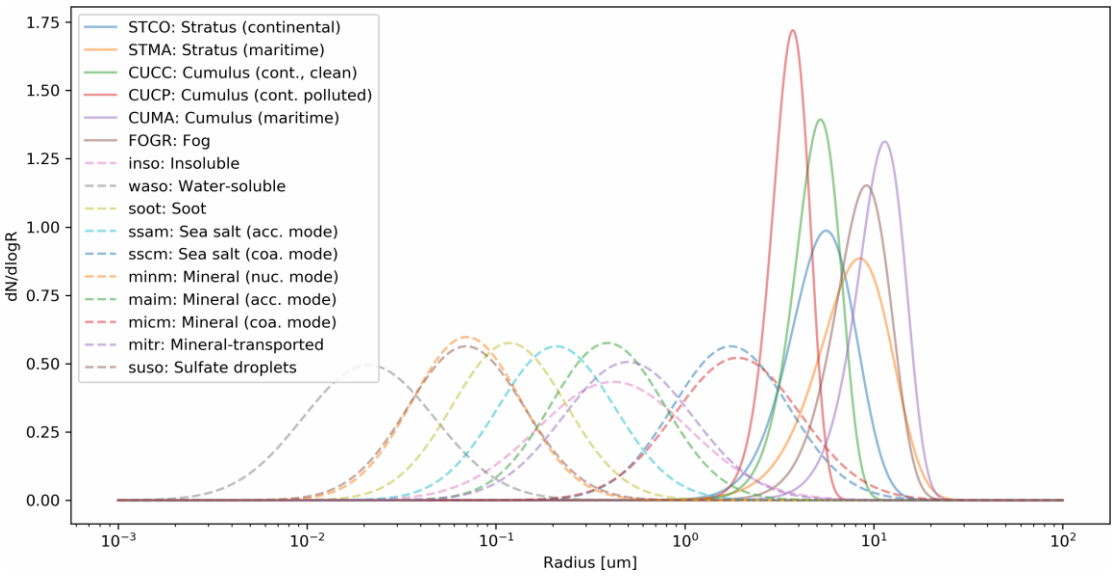

Figure 1:Number particle size distributions for aerosols (segmented lines) and clouds (solid lines) of the OPAC database.

The 1D-Var system is using an implementation of the L-BFGS- B algorithm for the minimization of the cost function. For this report, we have introduced the Levenberg-Marquardt minimizer in the cost function solver. This allows to solve the problem with both minimizers and keep the solution with smaller value of the cost function. This double solving approach is useful for runs where one of the solvers fails to converge successfully, which is frequently the case when the prior and the true value of the control are relatively distant. Because of the computational cost involved, this approach of double call to the minimizer is used in this report only with the aim of producing more confident solutions of the minimization, avoiding divert the discussion to issues related to the solver.

With the aim of evaluate the benefits of a second channel in the radiance assimilation, or to assess the performance of a control vector with cloud and aerosol variables, we have designed and performed a set of sensitivity test with synthetic observations. These tests include alternatives for the control vector and number of channels, but also different cases for

cloud and aerosols vertical profiles, while sampling the viewing and solar angles simulating a geostationary satellite. As a first step and during all the report, we have assumed an oceanic isotropic Cox-Munk reflectance model for all the simulations.

In these synthetic assimilation test, the true state of the atmosphere is known. As stated, we perform sensitivity tests mainly on the control vector definition and their values, as well as in the number of assimilated channels.

3.1 Control vector

In order to account for possible variations in the cloud and aerosols vertical distribution in the atmosphere, we have defined four cases for vertical profiles:

- Only aerosols (no clouds)
- Only clouds (no aerosols)
- Aerosols over clouds
- Clouds over aerosols

For the control vector, we have tested the assimilation for a joint control of cloud optical depth (COD) and aerosol optical depth (AOD), or only controlling the AOD (and assuming that the COD is known and equal the truth), or only controlling the COD (and assuming that AOD is known and equal to the truth).

All experiments use OPAC's maritime stratus (STMA) description for simulating the clouds size distribution and optical properties, as well as the "Industrial Absorbing" aerosol type form Escribano et al (GMD, 2018), which is a mixture of WASO (water-soluble), INSO (insoluble) and SOOT (soot) aerosol types from OPAC, with proportions (in particle number), by N_WASO=1200, N_INSO=0.1 and N_SOOT=8300. In the following figures, it is called "om". A summary of the cases regarding the selection of control variables and prescription of vertical profiles for clouds and aerosol is in Table 1.

Table 1: Experiment configuration. N(*x*,*y*) indicates a Gaussian vertical profile with mean *x* and standard deviation *y*, while exp(*H*) indicates an exponential profile with length scale of *H*

Experiment name	Aerosols in the atmosphere?	Aerosols in the control vector?	Clouds in the atmosphere?	Clouds in the control vector?	Vertical profile name	Vertical profile aerosols	Vertical profile clouds
only aerosols	yes	yes	no	no	only aerosols	exp(3000 m)	-
only clouds	no	no	yes	yes	only clouds		N(3500m, 300m)
clouds over aerosols control both	yes	yes	yes	yes	clouds over aerosols	exp(2000 m)	N(3500m, 300m)
clouds over aerosols control aerosols	yes	yes	yes	no	clouds over aerosols	exp(2000 m)	N(3500m, 300m)
clouds over aerosols	yes	no	yes	yes	clouds over aerosols	exp(2000 m)	N(3500m, 300m)

control clouds							
aerosols over clouds control both	yes	yes	yes	yes	aerosols over clouds	N(4000m, 300m)	N(1000m, 300m)
aerosols over clouds control aerosols	yes	yes	yes	no	aerosols over clouds	N(4000m, 300m)	N(1000m, 300m)
aerosols over clouds control clouds	yes	no	yes	yes	aerosols over clouds	N(4000m, 300m)	N(1000m, 300m)

Similarily to previous CAMS reports, and to Escribano et al. (2019), we have assumed a standard atmospheric profile (mid-latitude summer) with 49 vertical layers in the computations.

For each case, all the following combinations of prior AODs and CODs were computed (when applicable, following the cases of Table 1):

AOD: 0.01, 0.05, 0.184, 0.679, 2.5 (i.e., 5 values up to 2.5 equally log-spaced)

COD: 0.01, 0.1, 0.473, 2.236, 10.574, 50 (i.e., 6 values up to 50 equally log-spaced)

To produce enough flexibility to the control vector increments, we have set large errors for the prior error covariances. For both cases, AOD and COD, the diagonal element of the error covariance matrix is defined by a standard deviation of 0.4xOD+0.3. Error covariances between AOD and COD were neglected in these tests. While this choice of large errors in the B matrix is likely suboptimal for the standard data assimilation problem, it is desirable in this context because it shows the potential of assimilating this information in a system with large biases in the prior.

3.2 Observations

In line with previous works within the CAMS development framework, we have used the FLOTSAM radiative transfer model (RTM) in the observation operator and we have tested two radiative transfer models for computing the true TOA reflectances: FLOTSAM and DISORT. These true reflectances can be perturbed by Gaussian noise to compute the assimilated observations. Combined use of these capabilities of the 1D-Var allows us to distinguish four main subsets in terms of knowledge of modelling and observational system. When both, the true synthetic observations and the observation operator are the same (FLOTSAM), there is an implicit assumption of a perfect and unbiased observation operator. Computing the synthetic observations with a different RTM (DISORT) can exemplify the assumption of an imperfect observation operator, including systematic biases. (see the Appendix -- Section 0 -- for a simple comparison in the observational space) Adding random Gaussian noise (1%) to these observations can provide one of the experiments with plausible observational errors, while using a very small error (< 0.0001%) assumes that we know the modelling and observational systems. Therefore, four different experiments have been performed, by varying the RTM in the computation of the observed radiances (DISORT and FLOTSAM), and by perturbing these true radiances to obtain the observations (~1% error) or assuming a very small error (<0.0001% error). These values of the error description are also included in the observational error covariance matrix.

Viewing and solar geometries were estimated by sampling a geostationary viewing configuration for two dates (around boreal summer solstice and equinox: julian days 91 and 182), and for the following GMT hours: 4, 8, 12, 16 and 20. The sampled latitude-longitude points were selected to be approximately equidistant in the physical space. Figure 2 shows the used spatial sampling. From this set of space and time sampling, we discarded all those that with glint angle less than 40 degrees, or with viewing or solar zenith angle larger than 70 degrees.

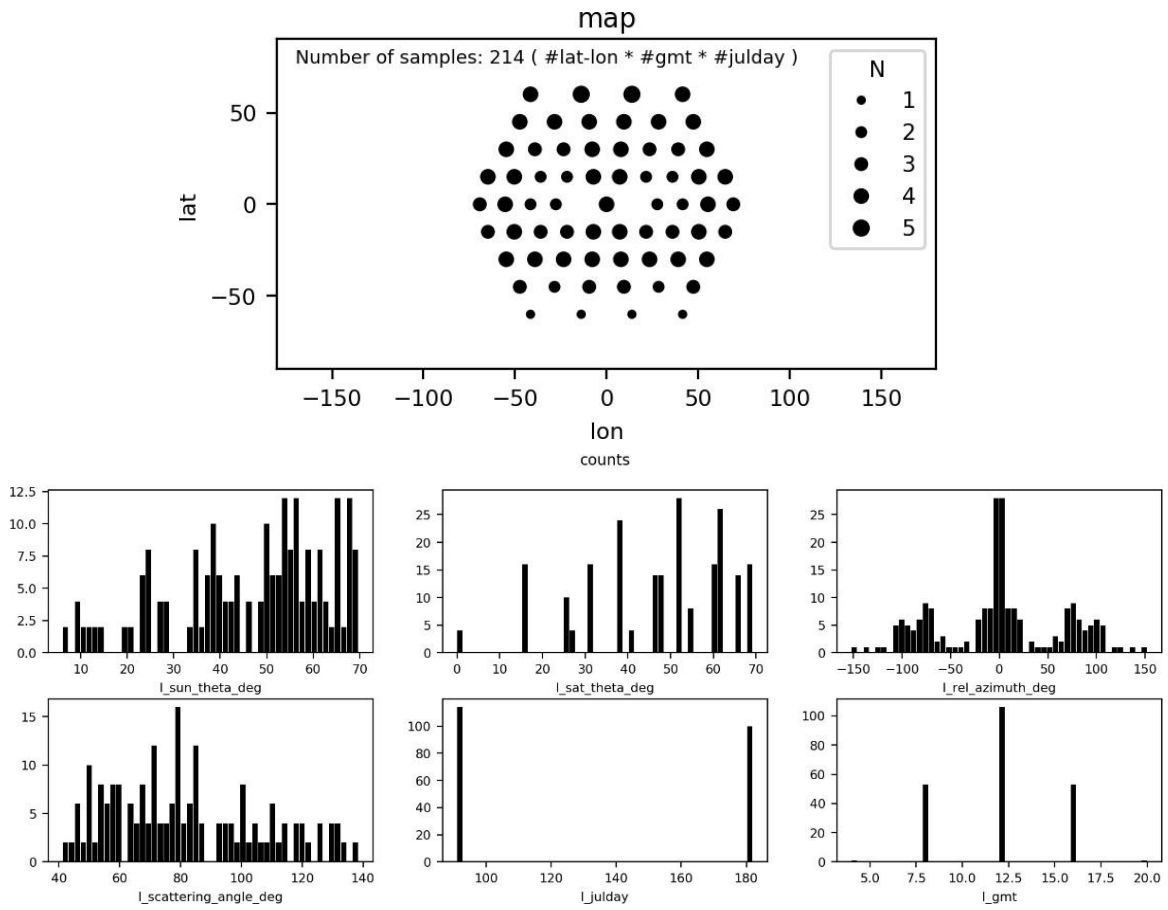

Figure 2: Spatial and temporal sampling of the solar and viewing geometry.

Figure 2 shows the distribution of the sampled solar and viewing azimuth angles (l sun theta deg and l sat theta deg panels), the relative azimuth angle (l rel azimuth deg) and the scattering angle (l scattering angle deg), computed from the selection of the latitude-longitude points, the two julian days and the GMT hours listed above. The subsatellite point was set to 0 degrees latitude and 0 degrees longitude.

In each assimilation experiment we consider two options:

- Only channel 660 nm is assimilated (“1 wavelength” experiments)
- Channels 660 nm and 865 nm are assimilated (“2 wavelengths” experiments)

For the case of 2 assimilated channels, we have set an error correlation of 0.6 between them in the observational error covariance matrix.

3.3 Scores and subset of experiments

Overall skills of the analyses were computed by a series of skill scores, including bias, mean fractional bias, mean fractional error, root mean square error, mean normalised bias, etc. Although the skill scores were computed for all experiments, in order to show the more relevant experiments, we have focused on the scores produced by a subset of all the experiments. This subset is defined by considering the priors of AOD and COD that are near to the true value of AOD and COD in the list of AOD and COD presented above. For example, if AOD true = 0.184, the subset will consider those experiment with AOD prior in {0.05, 0.184, 0.679}, as closest values of AOD from the {0.01, 0.05, 0.184, 0.679, 2.5} possibilities. The filtering on the prior AOD and COD is sound in the sense that usually data assimilation systems screen out observations with large departures prior to the minimization procedure. Scores used in this report are defined as:

$$\text{Root Mean Squared Error (RMSE)} = \sqrt{\frac{1}{N}\sum_{i=1}^{N}(m_i - r_i)^2}$$

$$\text{Mean Fractional Bias (MFB, MeanFracBias)} = \frac{2}{N}\sum_{i=1}^{N}\frac{m_i - r_i}{m_i + r_i}$$

$$\text{Mean Fractional Error (MFE, MeanFracError)} = \frac{2}{N}\sum_{i=1}^{N}\left|\frac{m_i - r_i}{m_i + r_i}\right|$$

$$\text{Mean absolute error (MeanAbsError)} = \frac{1}{N}\sum_{i=1}^{N}|m_i - r_i|$$

$$\text{Mean bias (MeanBias)} = \frac{1}{N}\sum_{i=1}^{N}m_i - r_i$$

$$\text{Mean normalised bias (MeanNormBias)} = \frac{1}{N}\sum_{i=1}^{N}\frac{m_i - r_i}{r_i}$$

$$\text{Model mean (ModelMean)} = \frac{1}{N}\sum_{i=1}^{N}m_i$$

with *r* the true value of the control variable, and *m* the value of the control (either prior or analysis). Number of samples is indicated by *N*. While during this report skill is exemplified with the Mean Fractional Bias and Mean Fractional Error, but the full set of scores is nevertheless shown in the summary figures of Section3.4.

4 Results

This section aims to summarize the main outcomes of the numerical experiments and it is organised by the definition of the control vector. Although all numerical experiments were performed, we present in detail only the results of the experiments with DISORT to compute the truth, observational error of 1% over the computed reflectance, and FLOTSAM model in the observation operator. We think that, as shown in the Appendix (Section 0) using two different solvers to compute the TOA reflectance introduces a systematic error in the system (which is usually undesirable in data assimilation and very common), but at the same time it would be more similar to a system working with real observation. In any case, the summary of scores of the other three options are presented in the Appendix (Section 6).

How to read the plots

We show the quality of the analyses in the control space, that is, by comparing the true value of the control variables (AOD and COD) with their analyses and prior counterpart. Experiments were performed by setting different values of the prior AOD and COD, as well as different values of the true AOD and COD. Qualitative assessment of the analyses is shown in histograms (or violin plots), exemplified in Figure 3.

Figure 3 indicates how to read the violin plots (or horizontal histograms) in this report. It is composed by a matrix of panels, with 2 histograms each. The true value of prescribed AOD and COD in the experiments are indicated in the x- and y-axis of the plot matrix and labelled in the left and top sides to the first panels. For each panel, two double histograms are provided, one for each variable in the control (AOD or COD). Histograms are produced by binning the analyses values of the experiments. Left side of the violin plots correspond to experiments were 1 channel (indicated as 1ch or 1 wavelength) is assimilated, while when 2 channels are assimilated, the histograms are indicated by “2ch” and plotted on the right side of the violin plots.

For each prescribed value of the true atmosphere AOD and COD (i.e., each individual panel of in Figure 3), the assimilation was performed with different values of the prior value of the control (which is also initial first guess of the cost function minimization). These different prior values are indicated by a cross and a horizontal line in the histogram panel, and their analyses histograms have the same color code. Please see examples on the annotations of Figure 3.

Figure 4 shows an annotated example of the scores plot used in this report for each of the studied cases. They are shown as heatmaps, that is, plots where the colors are associated to the values of the score of interest. In this report, the actual numerical value of the score is also annotated in the plots. As before, the true value of the AOD and COD are indicated in the x- and y-axis of the plot. The scores are computed for a subset of experiments: only those where the prior control value is close to the true value of the variable (c.f. Section 3.3 example).

For each pair of true COD and AOD values in Figure 4, there are four triangles (and values). As indicated in the Figure, the experiments where 1 satellite channel is assimilated are shown in the upper and left triangles (purple annotation), while those with 2 assimilated satellite channels are show in the lower and left triangles. We show also two different scores (c.f. Section 3.3) in these plots: Mean Fractional Bias (MFB) and Mean Fractional Error (MFE). MFB are annotated with blue color in Figure 4 and they are shown in bottom and left

triangles, while MFE are shown in upper and right triangles. In summary, the possible combinations are:

- Upper triangles: MFE for the 1 channel assimilation experiments
- Right triangles: MFE for the 2 channel assimilation experiments
- Left triangles: MFB for the 1 channel assimilation experiments
- Bottom triangles: MFB for the 2 channel assimilation experiments

The color scales of the two scores (MFB, MFE) are shown in color bars on the right of the Figure. MFE is a normalised score in the [0,2] range that is shown with brown range of colors, being the zero value the best MFE score possible (in while). MFB is shown with blue and red colors. Best MFB is achieved with zero value (white) and it is also normalised in the [-2,2] range.

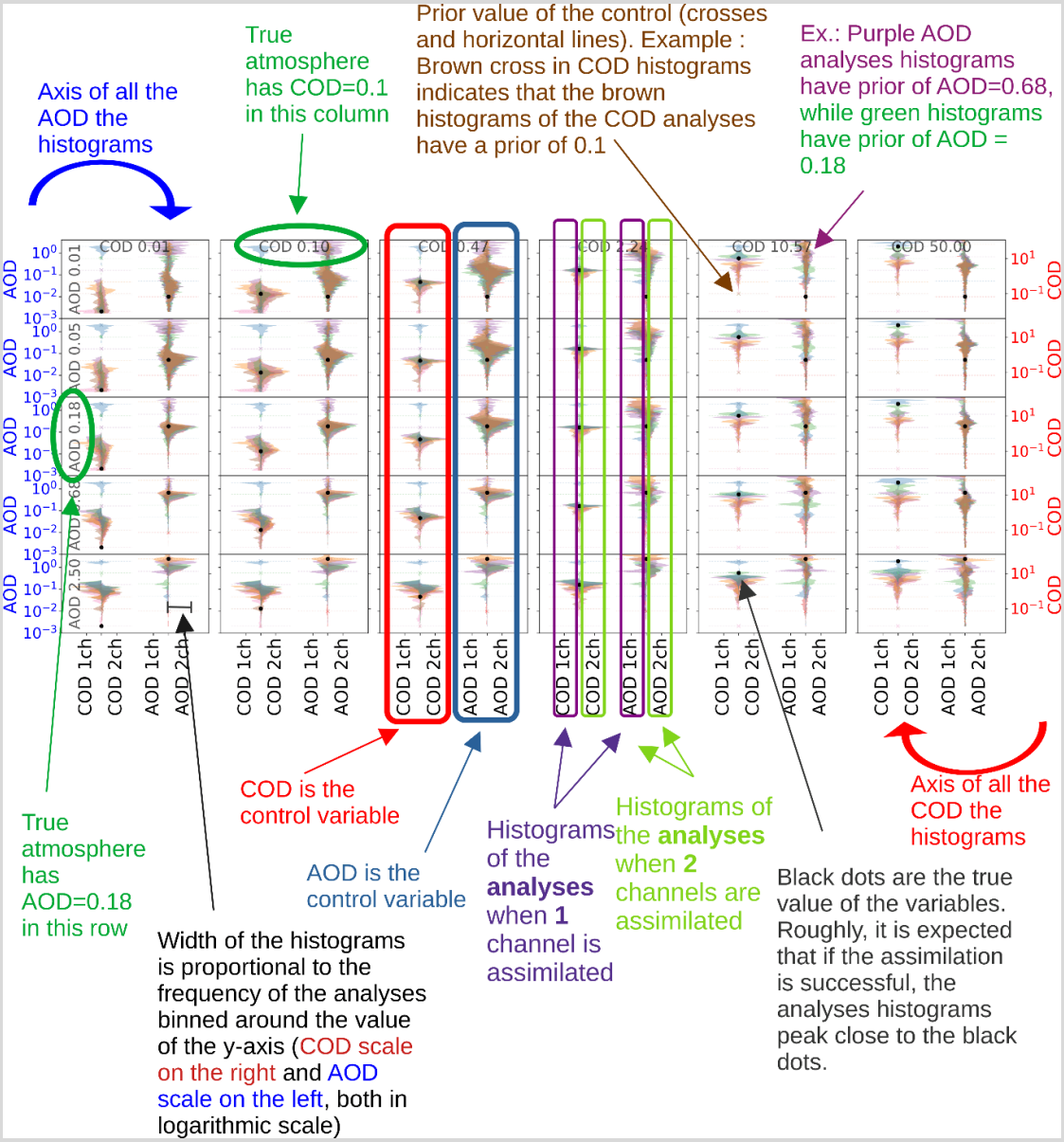

Figure 3: Annotated histogram example.

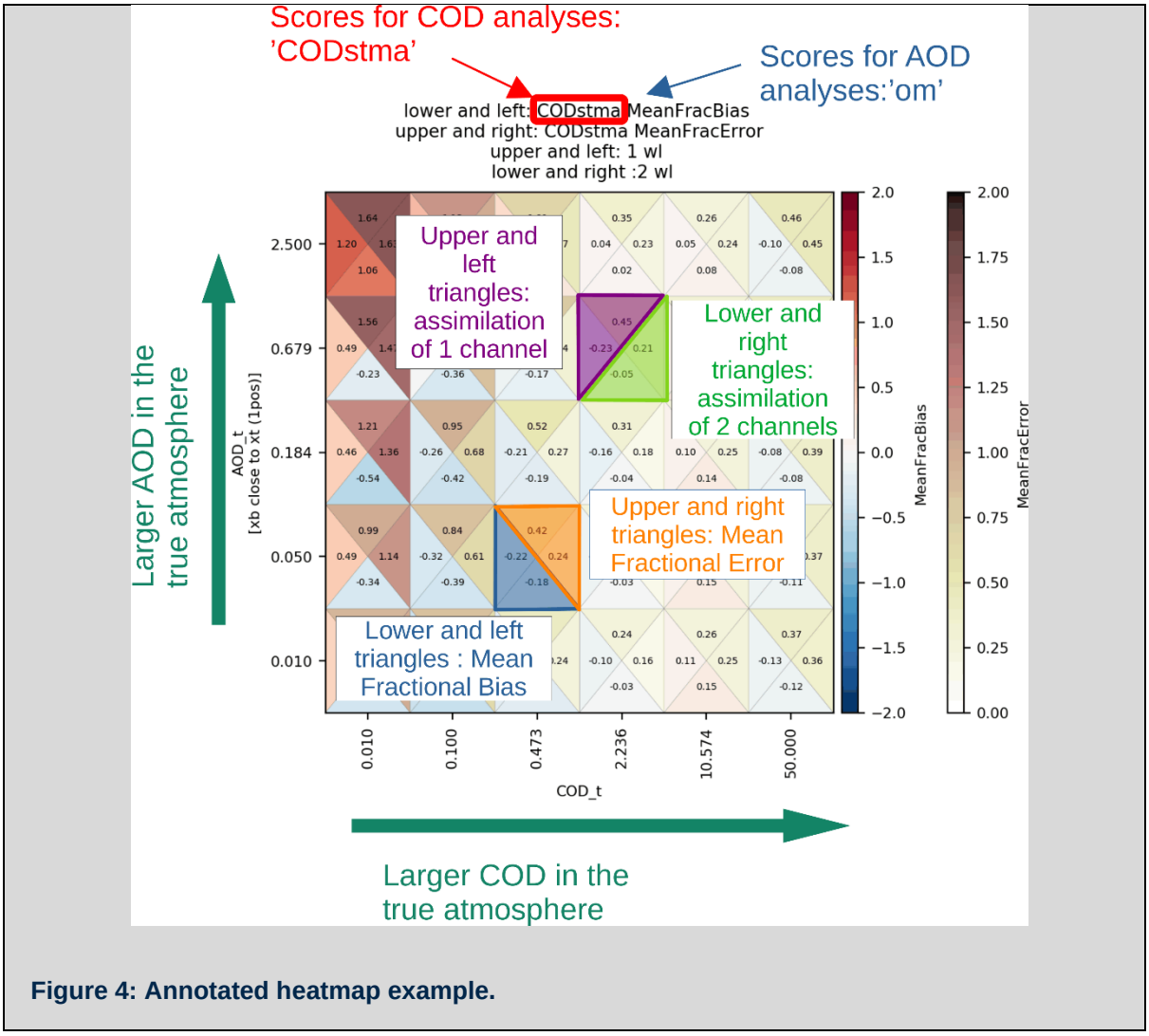

Figure 4: Annotated heatmap example.

4.1 Only COD in the control vector

4.1.1 Atmosphere with clouds, no aerosols

Figure 5 shows the analyses of COD when only clouds are present in the atmospheric column (case only clouds). Panels are for different values of the true COD (black dots), while the histograms indicate the COD analyses. These are tagged by their corresponding prior COD. Histograms on the left of the central axis of each panel are the analysis for experiments that uses only one channel in the assimilation, while experiments using two channels are shown on the right. Qualitatively, closer the prior (in colours and colour crosses) implies a better analysis, and the two-channel assimilation perform better than the assimilation with one channel only.

More quantitatively, Figure 5 shows the Mean Fractional Bias (MFB) and Mean Fraction Error (MFE) of the analyses with respect to the truth, for the cases where the prior is close to the truth, as explained before. Similarly to the previous Figure, the two-channel ("2ch" or "2wl") experiments perform better that those with only one channel assimilated. These scores also perform better for larger values of COD.

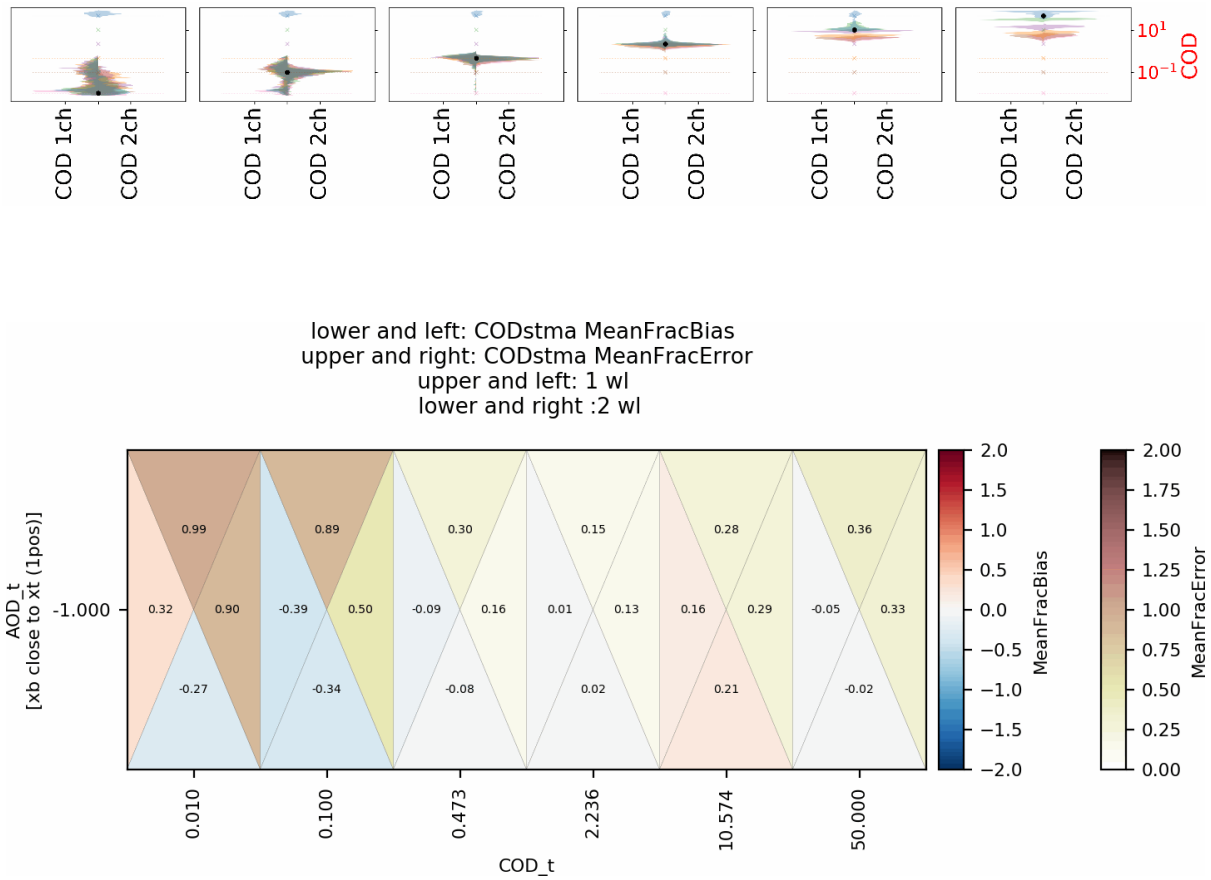

Figure 5: Histograms and scores for the case of only clouds. Top panel shows histograms of COD analyses for the six prescribed values of the truth COD (columns). True COD value is shown with black dots. Coloured histograms indicate analyses issued for experiments with different (corresponding) coloured value (crosses). Histograms on the left were produced with the assimilation of one channel, and two channels on the right. Please note the logarithmic scale on the top panel. Bottom panel shows the Mean Fractional Bias (MFB, lower and left triangles) and Mean Fractional Error (MFE, upper and right triangles) for the case of one channel assimilation (upper and left triangles) and two channels (lower and right triangles). AOD is not prescribed (therefore it appears with an invalid value, -1 in the plots).

4.1.2 Atmosphere with aerosols over clouds

Similar histograms of analyses are show in Figure 6. In this case, the columns show experiments with different values of the true COD (increasing to the right, as show in the label on top of each panel), while in the increase of the true AOD values are increasing in the rows (as shown in the labels on the left of the panels in the first row). As before, the 2-channel assimilation outperforms the one with one channel. For a fixed value of COD, it seems that the quality of the analyses decreases with the increase of the aerosol load (AOD). For low AOD and COD, the observation operator (c.f. plots in Section 0) error might contribute to the low accuracy, with respect to larger OD values.

The degradation of MFB and MFE scores are while increasing AOD is also clear in Figure 6. Please note that the order of the rows are inverted in this figure, so best scores are in the lower and middle rows, while they worsen in the upper rows for large AODs. As in the case without aerosols, best normalised scores are found for large values of COD (i.e., stronger signal at the top of the atmosphere)

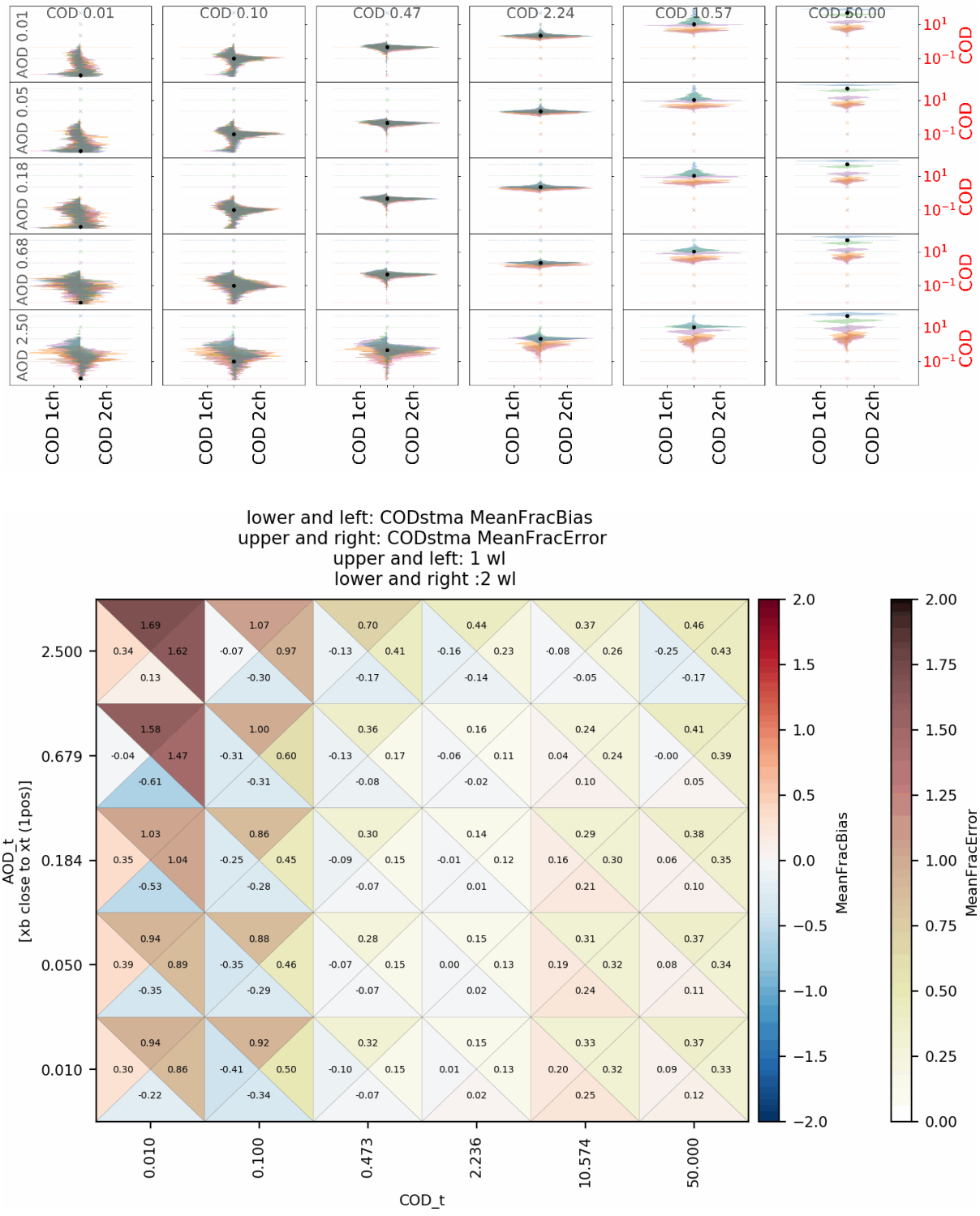

Figure 6: Histograms and scores for the case of aerosols over clouds, but only COD in the control vector. Similar to Figure 5 but for different values of aerosol load (AOD, rows) in each panel.

4.1.3 Atmosphere with clouds over aerosols

Figure 7 shows histograms for the case where clouds are above aerosols. The only noticeable difference with the previous case happens when AOD is large. There, the analysis COD show better scores (and for, in addition, large COD).

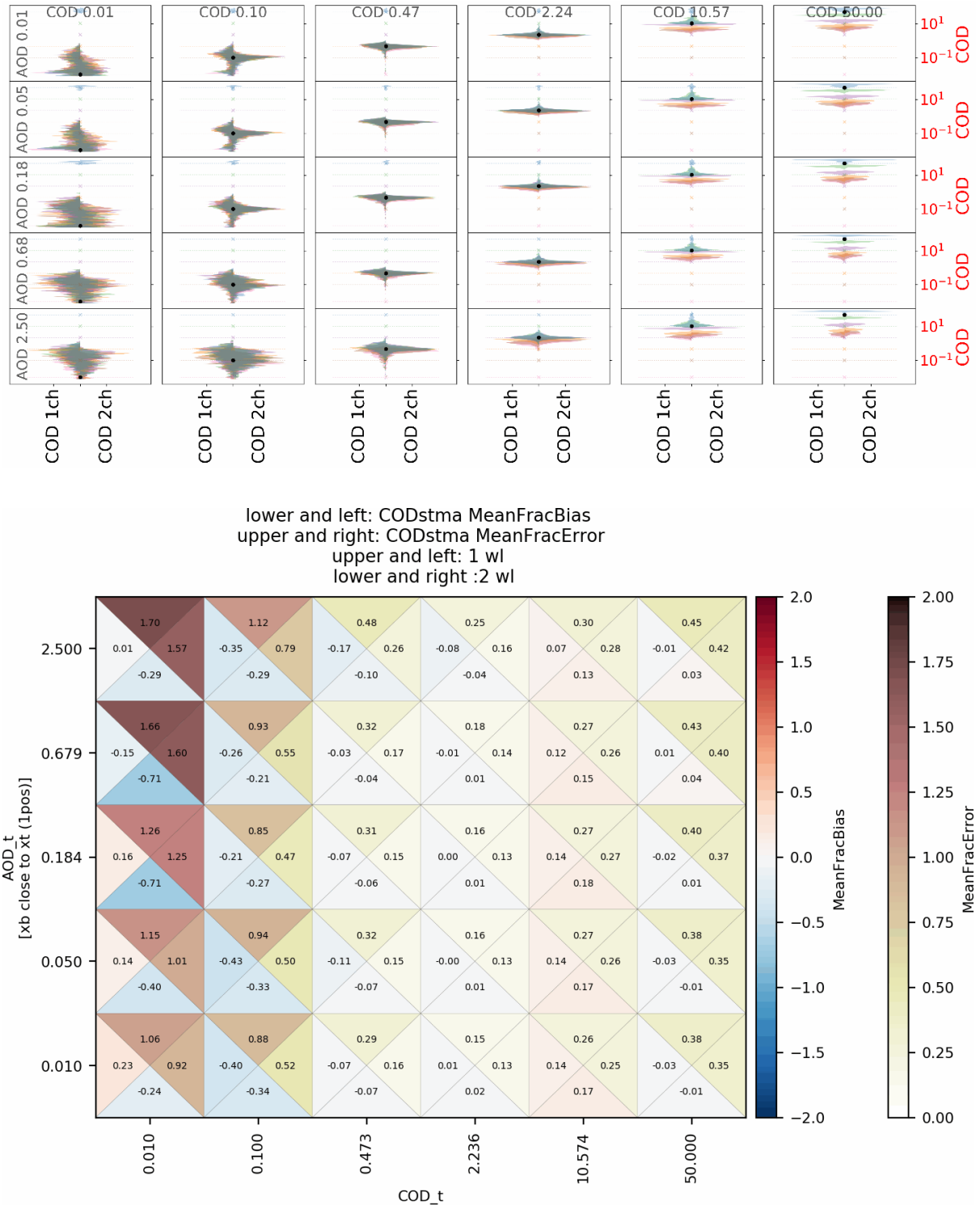

Figure 7: Histograms and scores for the case of clouds over aerosols, but only COD in the control vector. Similar to Figure 6.

4.2 Only AOD in the control vector

4.2.1 Atmosphere with aerosols, no clouds

Figure 8 shows the analyses histograms for the case where only aerosols are present. In the same way as the case with only clouds, the 2-channel assimilation show better qualitative analyses than the 1-channel counterpart. MFE is also better in the 2-channel assimilation, but MFB is most of the time worst in the 2-channel assimilation. Also, it shows, in general, better scores for large values of AOD.

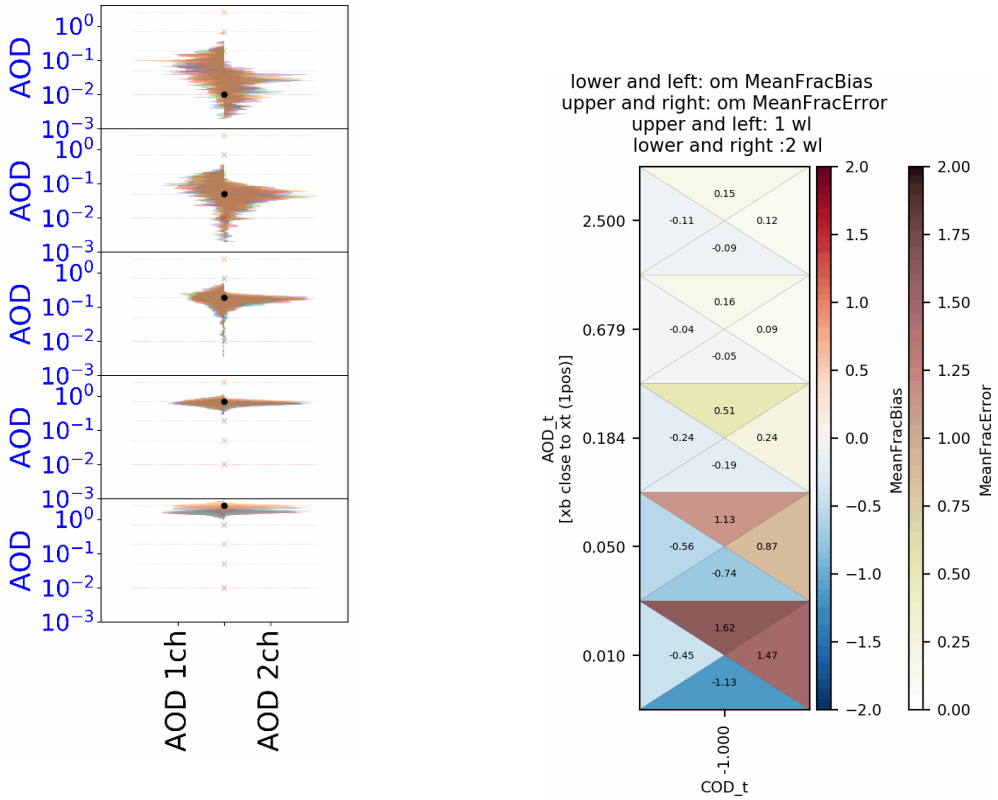

Figure 8: Histograms and scores for the case of only AOD in the atmosphere and in the control vector (that is, COD=0). Left panels show the histograms of analyses the right panel show their MFB and MFE scores.

4.2.2 Atmosphere with aerosols over clouds

Figure 9 show the histograms for the AOD analyses and their MFE and MFB scores. In this case, the 2-channel assimilation show better MFE and MFB in most of the plots. Scores are better for large values of AOD, and for small values of COD.

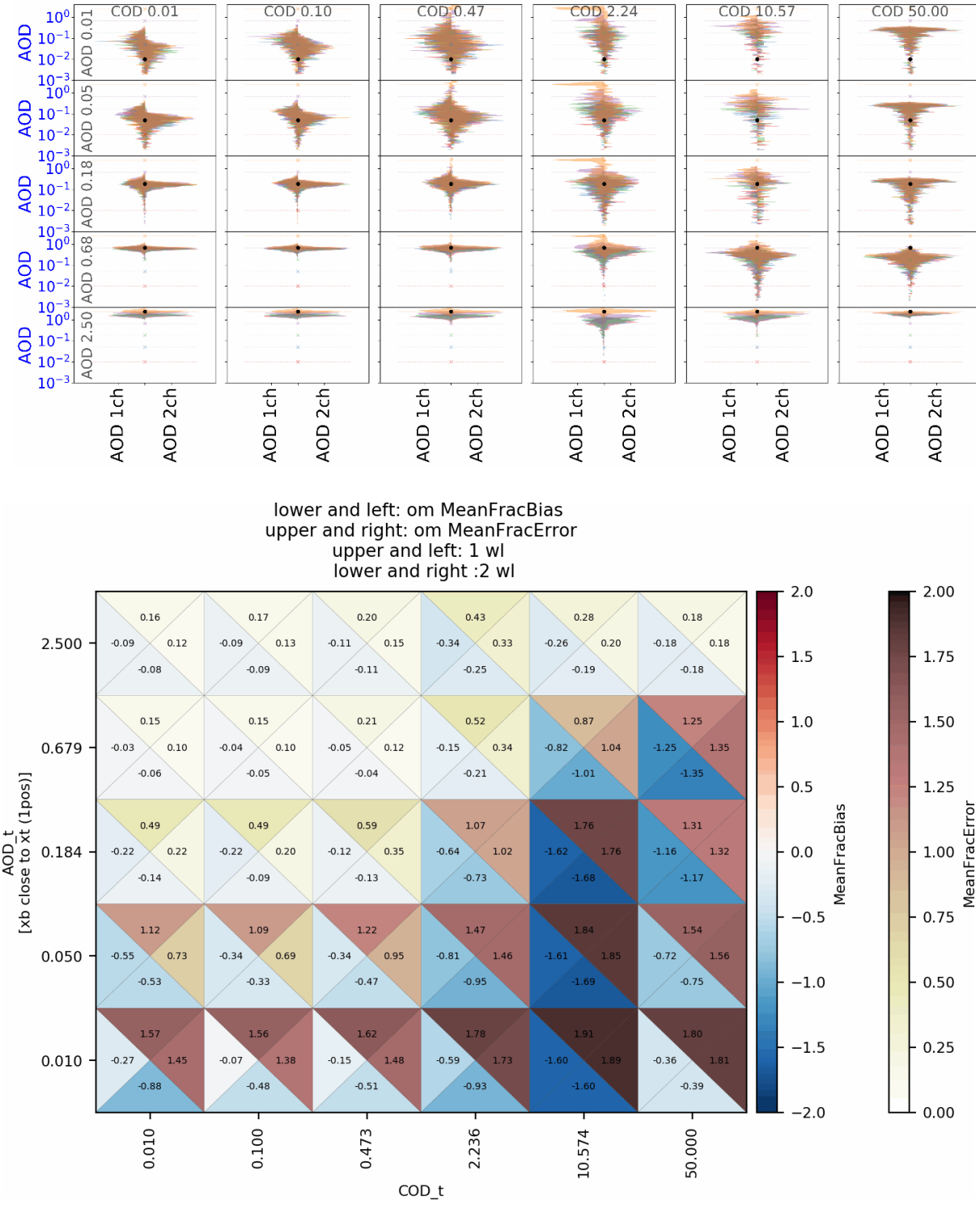

Figure 9: Histograms and scores for the case of aerosols over clouds, but only AOD in the control vector. Similar to Figure 8 but for different values of cloud thickness (COD, columns) in each panel.

4.2.3 Atmosphere with clouds over aerosols

As clouds are above aerosols, a thick cloud layer decreases the sensitivity of detecting the effect of aerosols in the reflected sunlight. Histograms and scores (Figure 10) for cases with

COD>10 show that the system is not able to improve the prior estimates significantly. For lower values of COD, the analysis improves the scores only if the aerosol signal is strong enough to be seen below the cloud.

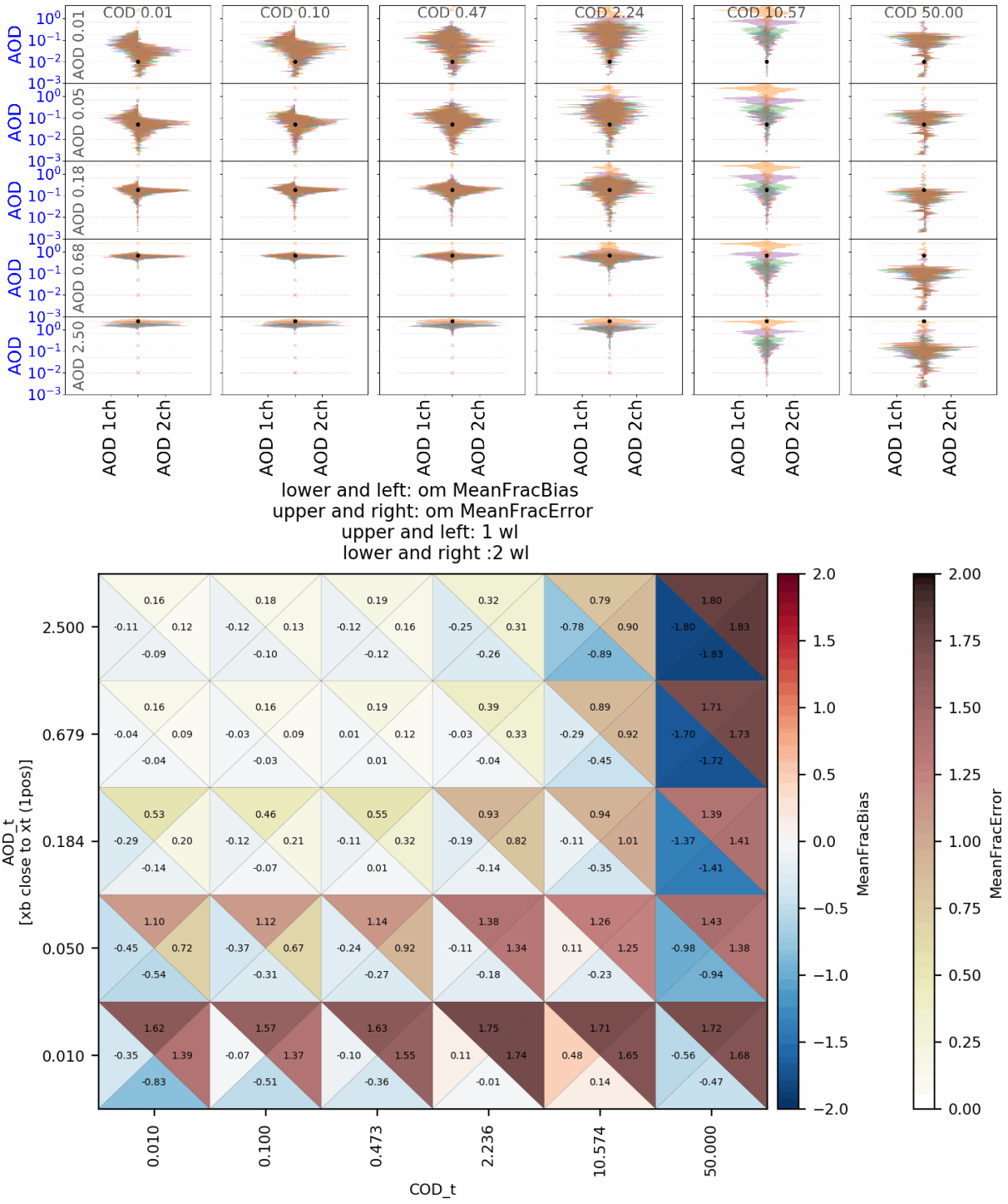

Figure 10: Histograms and scores for the case of clouds over aerosols, but only AOD in the control vector. Similar to Figure 9.

4.3 Joint control of AOD and COD

The following experiments contain both, aerosols and clouds in the atmosphere and in the control vector, meaning that now the system must estimate two variables at once, but using reflectances from one or two channels. In general, it is not expected that the system shows better analyses scores than the cases showed before, in particular for the 1-channel assimilation. As before, we show two cases, aerosols over clouds, and clouds over aerosols.

4.3.1 Atmosphere with aerosols over clouds

Although in Figure 11 the histograms of analyses show a large spread and low accuracy with respect to the previous cases, the improvement with respect to the prior (colour cross and horizontal line in the plots) is noted. MFE and MFB shows better scores for COD when the true COD is relatively large and AOD is low. Conversely, AOD analyses skills are better when COD is low and AOD is large.

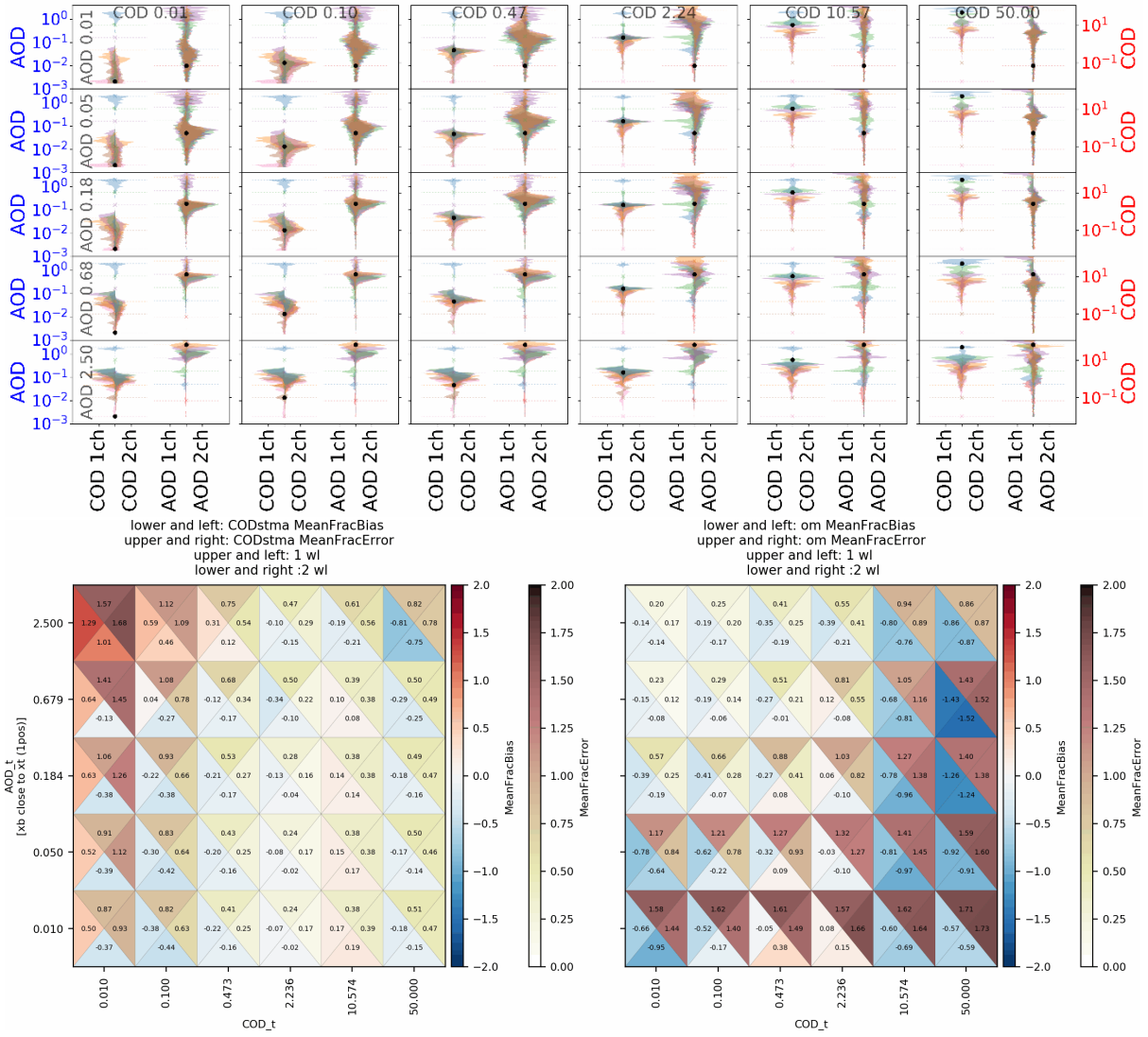

Figure 11: Histograms and scores for the case of aerosols over clouds, with COD and AOD in the control vector. Each panel in the two upper figures contains two groups of histograms, for COD on the left and for AOD on the right.

4.3.2 Atmosphere with clouds over aerosols

In an atmosphere where clouds are above aerosols, Figure 12 shows results very similar to those of the previous case, but with some degradation in the AOD analyses scores in case of large COD; and a small improvement of COD scores for large AOD values of the truth.

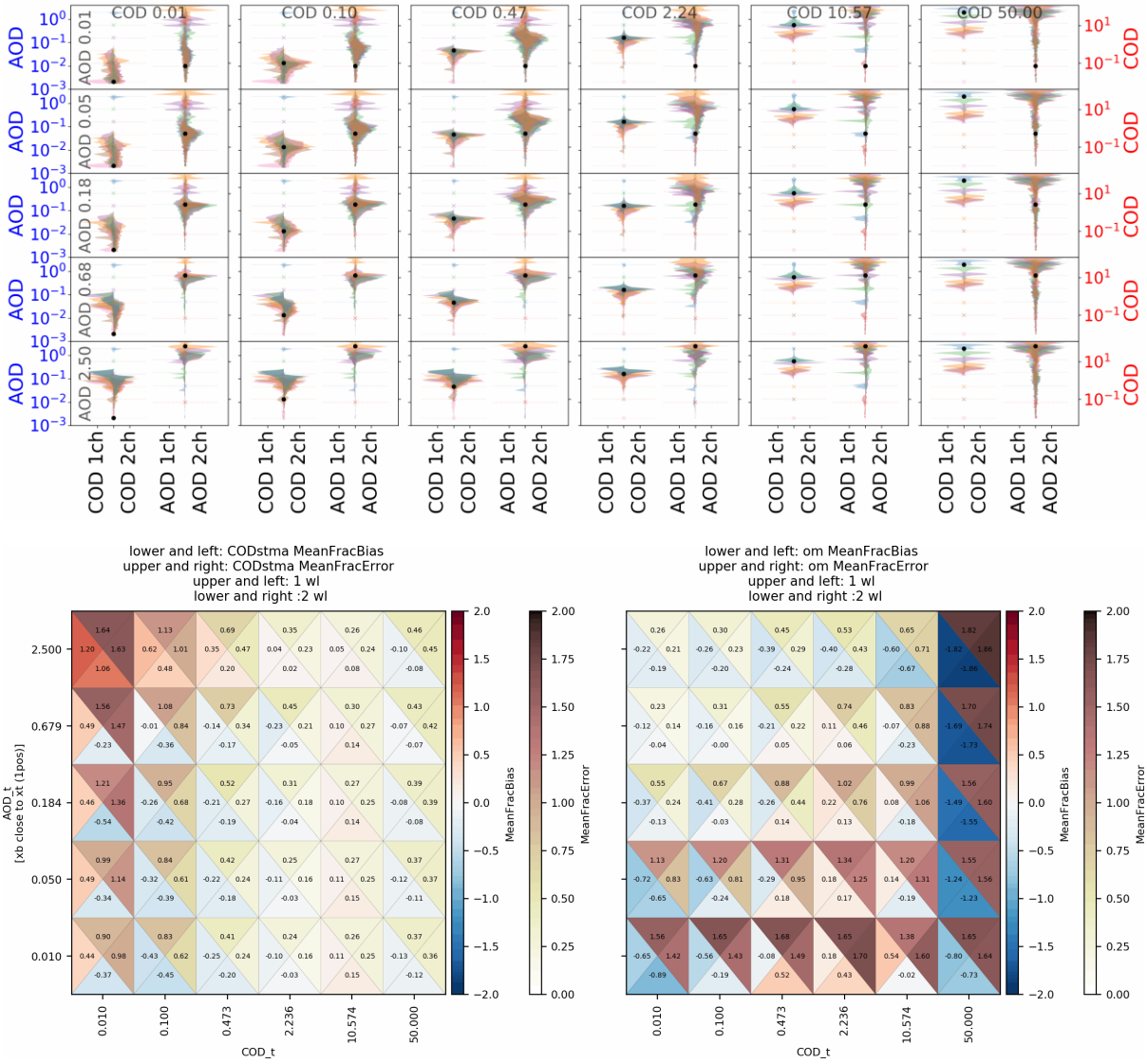

Figure 12: Histograms and scores for the case of clouds over aerosols, with COD (left) and AOD (right) in the control vector.

4.4 Summary of scores

In order to produce meaningful results, we have computed the scores for the experiment where the prior is close to the true values (see section 3.3 for details). This filtering is in practice similar to common practices for data screening in data assimilation systems, where outliers (with respect to the prior) are discarded before the assimilation procedure under certain conditions. We have computed the values of all the metrics defined in Section 3.3, and

we present them in the following Figures. Figure 13 show the scores of the prior, Figure 14 those from the analyses and Figure 15 shows the ratio between those two values, that is the analyses scores divided by the prior scores.

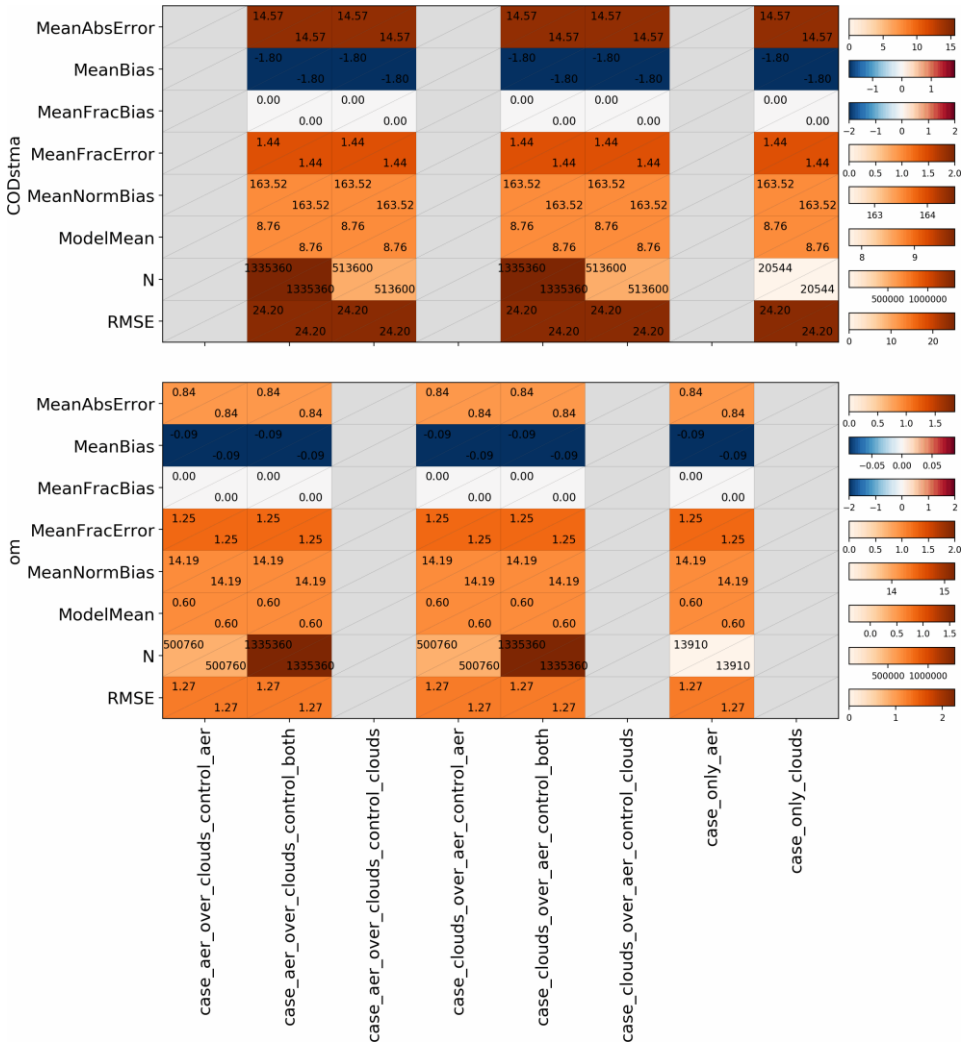

Figure 13: Scores of the prior for all the experiments. Upper panel show the scores for the COD control vector element and lower panel those of AOD. Experiments are indicated in columns and scores in rows.

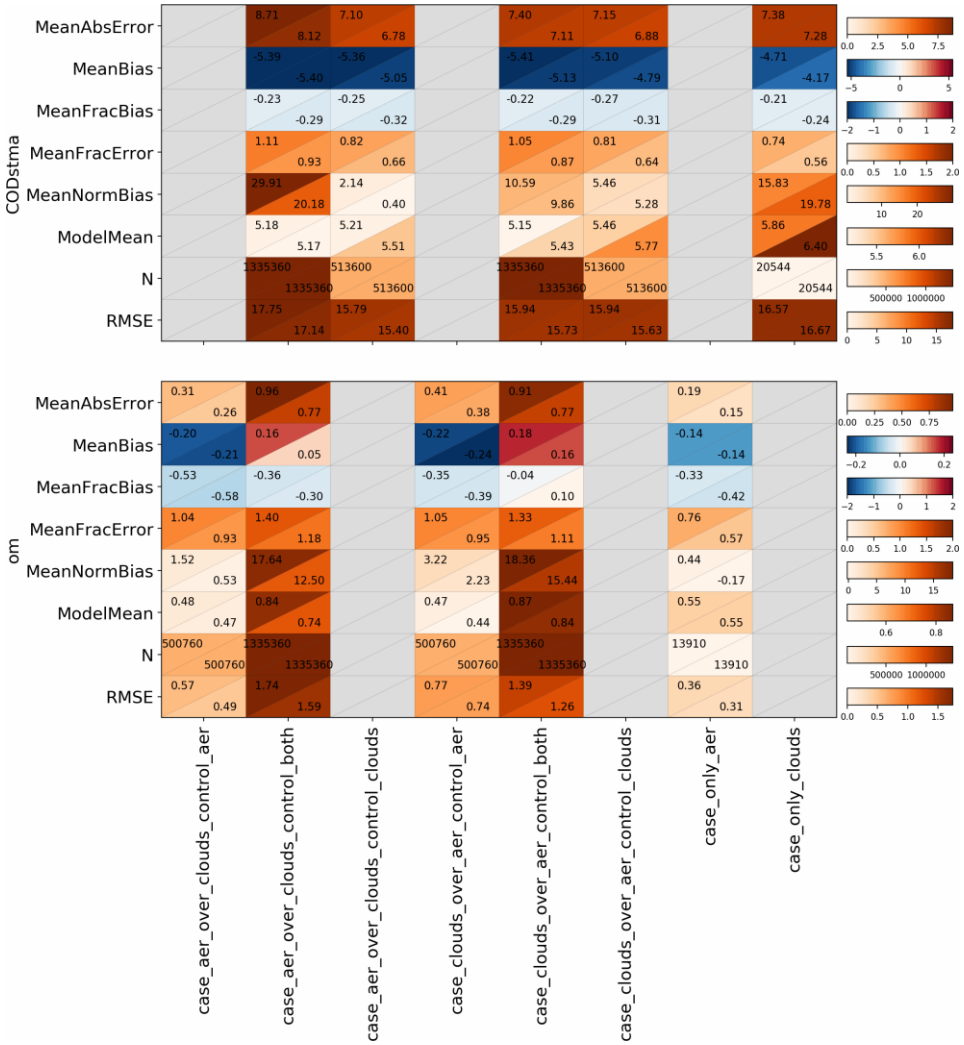

Figure 14: Scores of the analysis for all the experiments. Upper panel show the scores for the COD control vector element and lower panel those of AOD. Experiments are indicated in columns and scores in row.

Experiment design determines the values of Figure 13, including the filter for prior close to the truth. Also by design, the scores are constant across experiments, except by the number of experiments, that depends on the possible options of the atmospheric column composition and the control vector (AOD, COD, or both). Figure 13 should be only interpreted in context with Figure 14, as it is the starting point to estimate potential benefits of the assimilation.

Figure 14 shows the scores for the experiment analyses, while Figure 15 shows the ratio between prior and posterior (analyses) scores. In this last Figure, error scores, where the best values scores zero (like MFE, mean absolute error, RMSE), values less than he unity (in blue tones) shows an improvement after assimilation. Mean normalised bias is generally decreased after assimilation while mean bias is increased. Because the prior set is symmetrical (in log-scale by design of the COD and AOD cases) with respect to the truth, MFB is zero so an increase of this score for the analysis is expected (and the ratio of Figure 15 equal infinity). Error measures like RMSE, mean absolute error and mean fractional error are, in general, improved after assimilation.

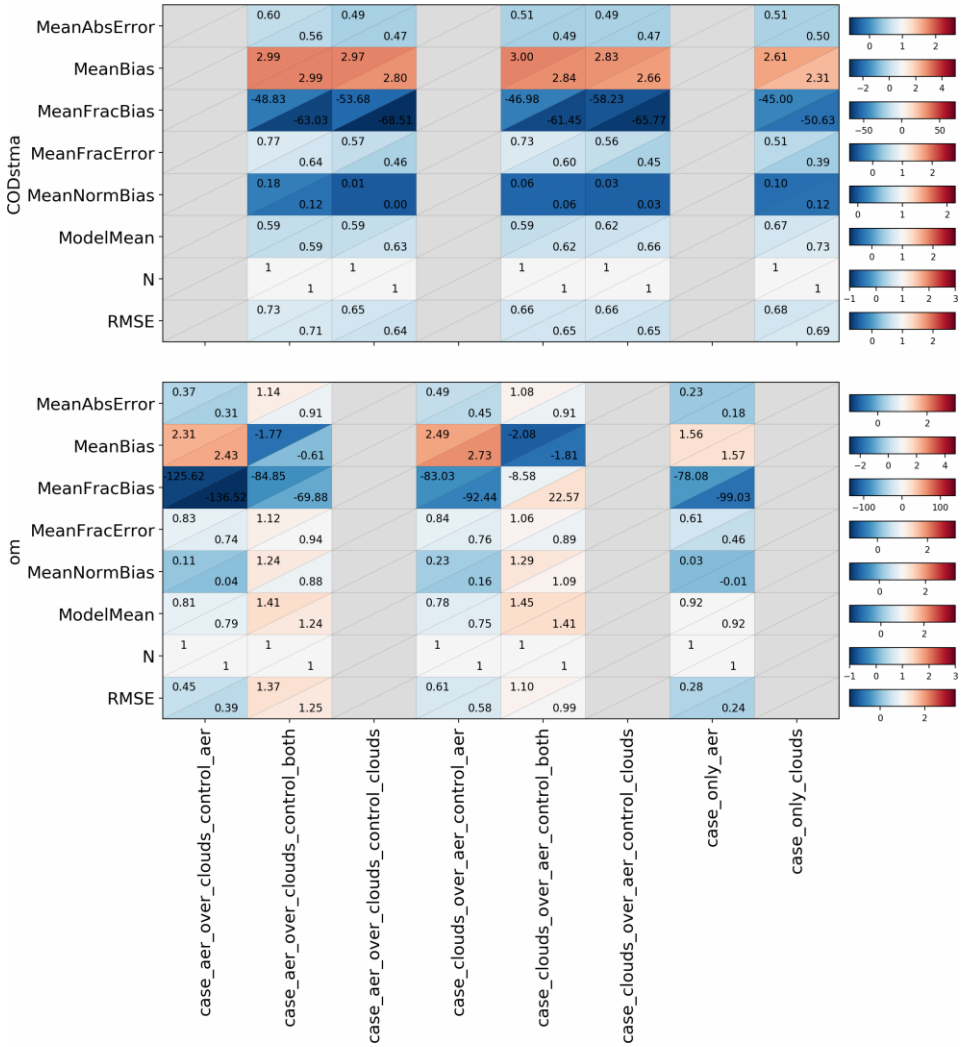

Figure 15: Ratio of scores (i.e., scores of the analysis divided by the scores of the prior) for all the experiments. Upper panel show the scores for the COD control vector element and lower panel those of AOD. Experiments are indicated in columns and scores in rows. White colour is assigned to the values equal one, blue to values smaller than one (score of analysis is smaller than the score of the prior), and red to values larger than one (score of the analysis is larger than the score of the prior).

There is a clear gain when the second channel is added in almost all experiments and cases. Moreover, this is necessary for improving scores when the two variables are controlled: the one-channel assimilation degrades most of the error scores with respect to the prior.

Without surprise, the best scores are reached for cases when only one variable is present in the atmosphere and in the control vector, that its, “only clouds” case for COD scores and “only aer” for AOD. In cases of atmospheres with both, aerosols and clouds, best scores are reached, again, when only one variable is in the control vector (while the other is assumed to be known perfectly). Here, errors are smaller when the control variable is on the upper atmospheric layer, as “clouds over aerosol” for COD assimilation and “aerosol over clouds” for AOD assimilation. Cases where the two variables are in the control vector are, as expected, the ones providing overall worst scores because none of the variables is assumed to be known and equal to the truth. Here, and similarly to the other cases, best scores are reached for each variable when the variable is in the upper part of the atmosphere: for AOD, “aerosol over

clouds" provide better scores than "clouds over aerosol", while "clouds over aerosol" provides better COS scores than "aerosol over clouds".

5 Conclusion

We have designed and performed a series of test for supporting the implementation of short-wave radiance assimilation for aerosols and clouds. The tests were done with a 1-dimensional 1D-Var assimilation system, under ideal conditions over ocean. We have computed the synthetic observations with a radiative transfer model different from the one used in the observation operator. Experiments were designed for cases were a type of cloud and a type of aerosol were present in the atmosphere with ranging values and proportions, while controlling cloud optical depth and aerosol optical depth jointly or separately. We have assumed perfect knowledge on the surface reflectance model, the aerosol and cloud types and their vertical profile and the atmospheric and molecular vertical profile. Experiments were produced using a sample of idealised viewing angles from a geostationary satellite and using either one or two visible channels as input data for the assimilation.

Best scores were obtained when the experiment was less complex (aerosols with no clouds, or clouds with no aerosols). When both, AOD and COD are present, the strength and vertical distribution of them impacts the quality of the analyses.

For cases with clouds and aerosols the two-channel assimilation show better analyses scores than the one-channel assimilation. Moreover, when AOD and COD are in jointly estimated, the one-channel assimilation might degrade scores with respect to the prior, while the two-channel assimilation show improved skills.

It is expected that a full 4D-Var system will outperform the 1D-Var used here. The assimilation of a second (or 3rd) visible channel is desirable, and the joint control of AOD and COD have potential to improve analyses in the most favourable cases (medium, low or null COD; and medium and strong AOD) when only shortwave reflectances are assimilated. The addition of shortwave information to assimilation of other cloud or aerosols sensitive could, in principle, work synergistically for improving the quality of cloud and aerosols analyses.

6 Appendix 1: Summary plots for other configurations

6.1 RTM truth: DISORT, observation operator: FLOTSAM, 0.000001% obs. error

Summary of scores for this case are in Figure 16 and Figure 17.

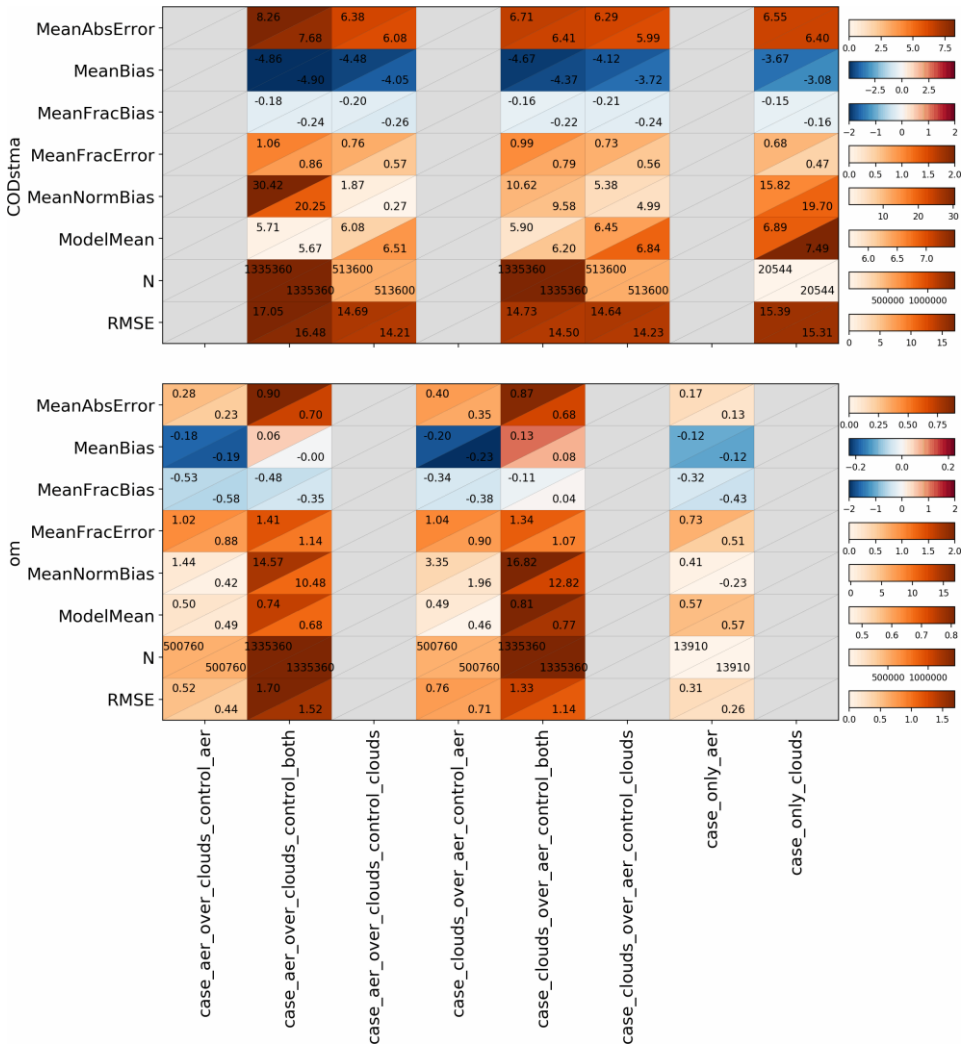

Figure 16: Similar to Figure 14 but without adding random noise to the simulated observations.

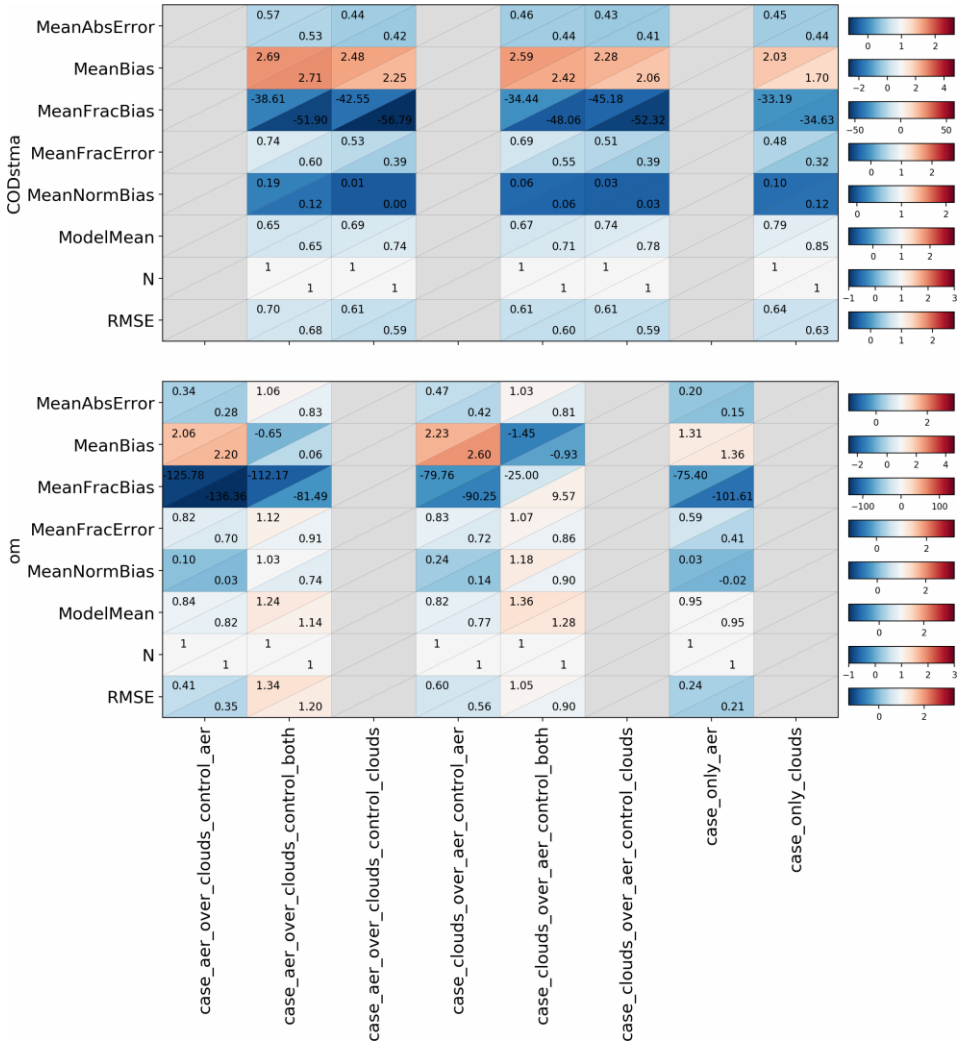

Figure 17: Similar to Figure 15 but without adding random noise to the simulated observations.

6.2 RTM truth: FLOTSAM, observation operator: FLOTSAM, 1% obs. error

Summary of scores for this case are in Figure 18 and Figure 19.

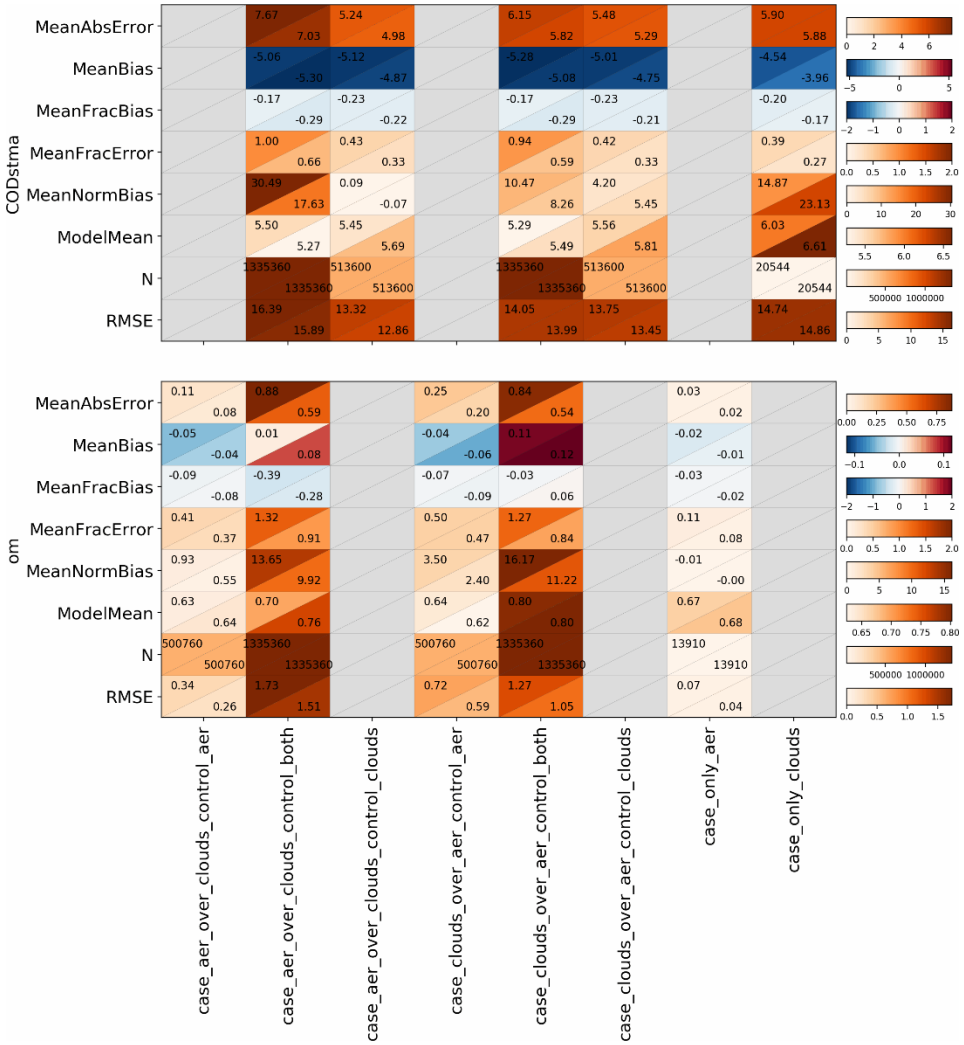

Figure 18: Similar to Figure 14 but using FLOTSAM as radiative transfer model for the true atmosphere.

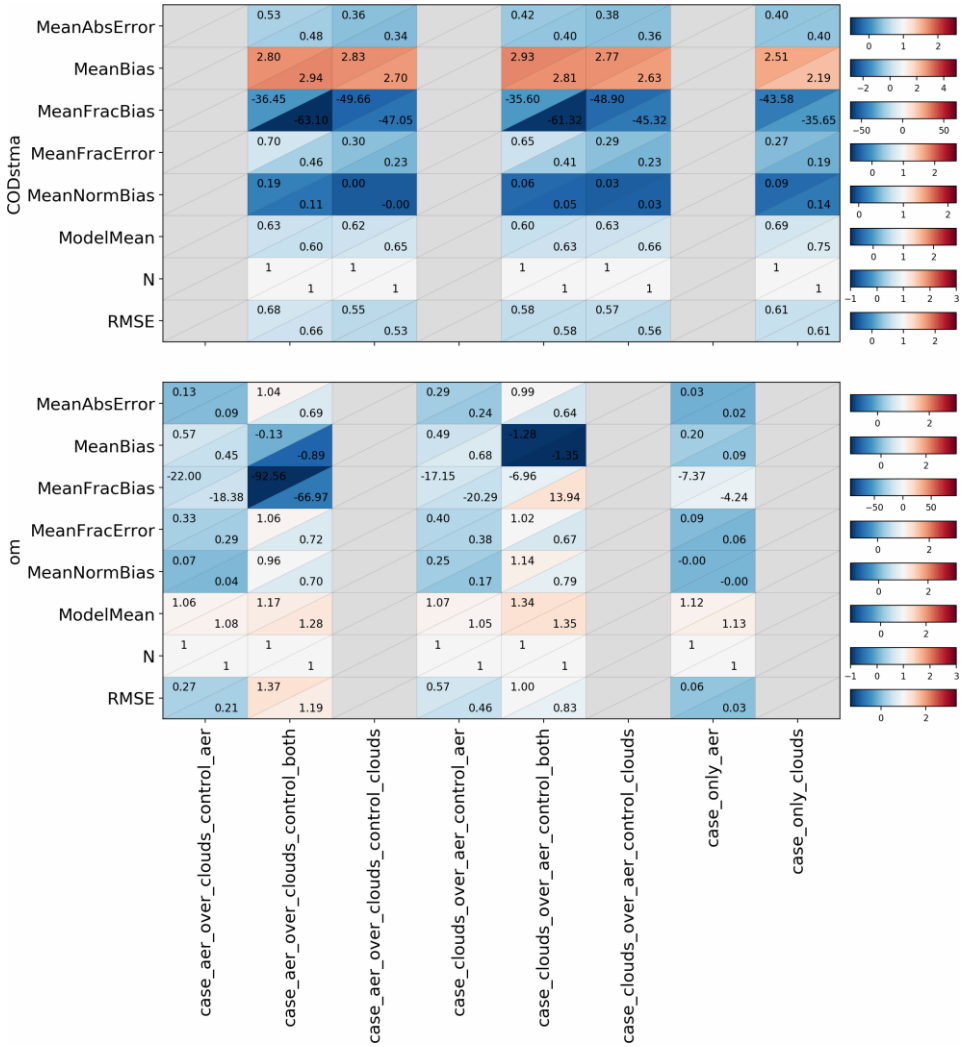

Figure 19: Similar to Figure 15 but using FLOTSAM as radiative transfer model for the true atmosphere.

6.3 RTM truth: FLOTSAM, observation operator: FLOTSAM, 0.000001% obs. error

Summary of scores for this case are in Figure 20 and Figure 21.

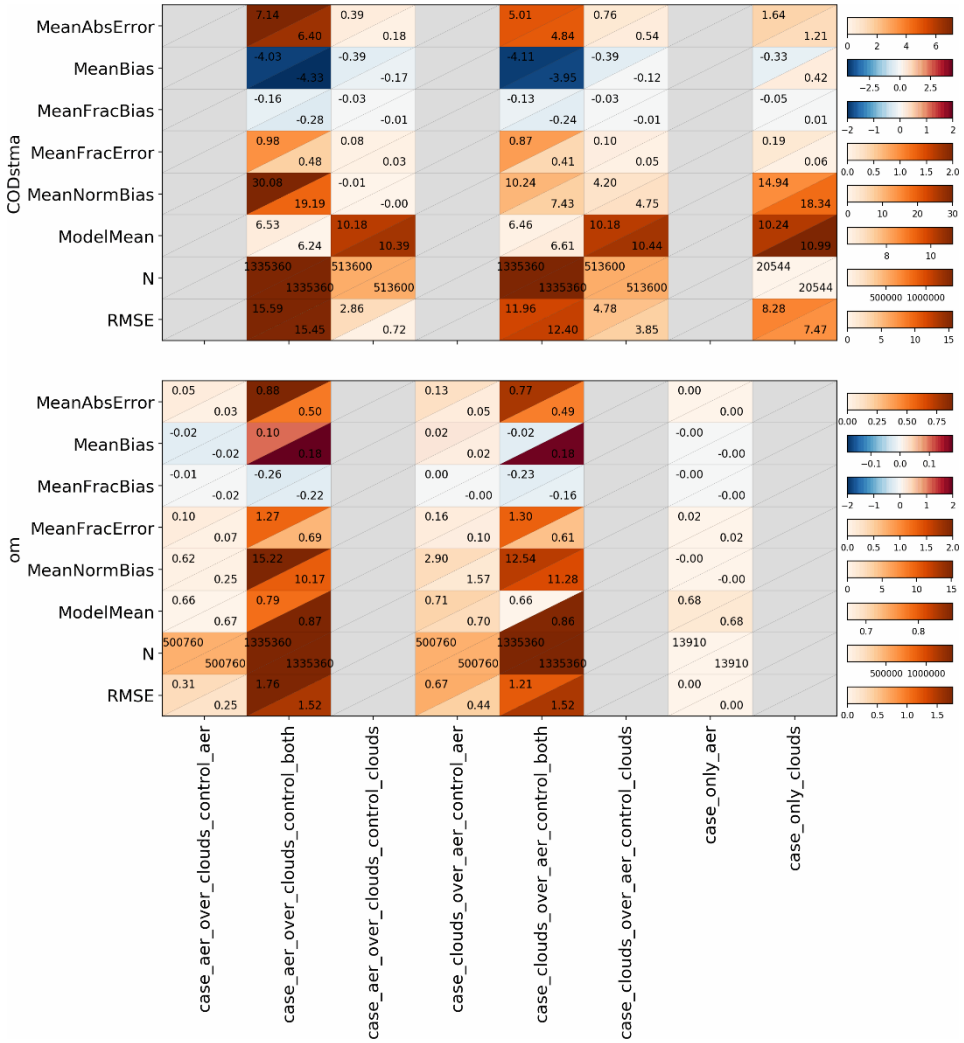

Figure 20: Similar to Figure 14 but using FLOTSAM as radiative transfer model for the true atmosphere and without adding random noise to the simulated observations.

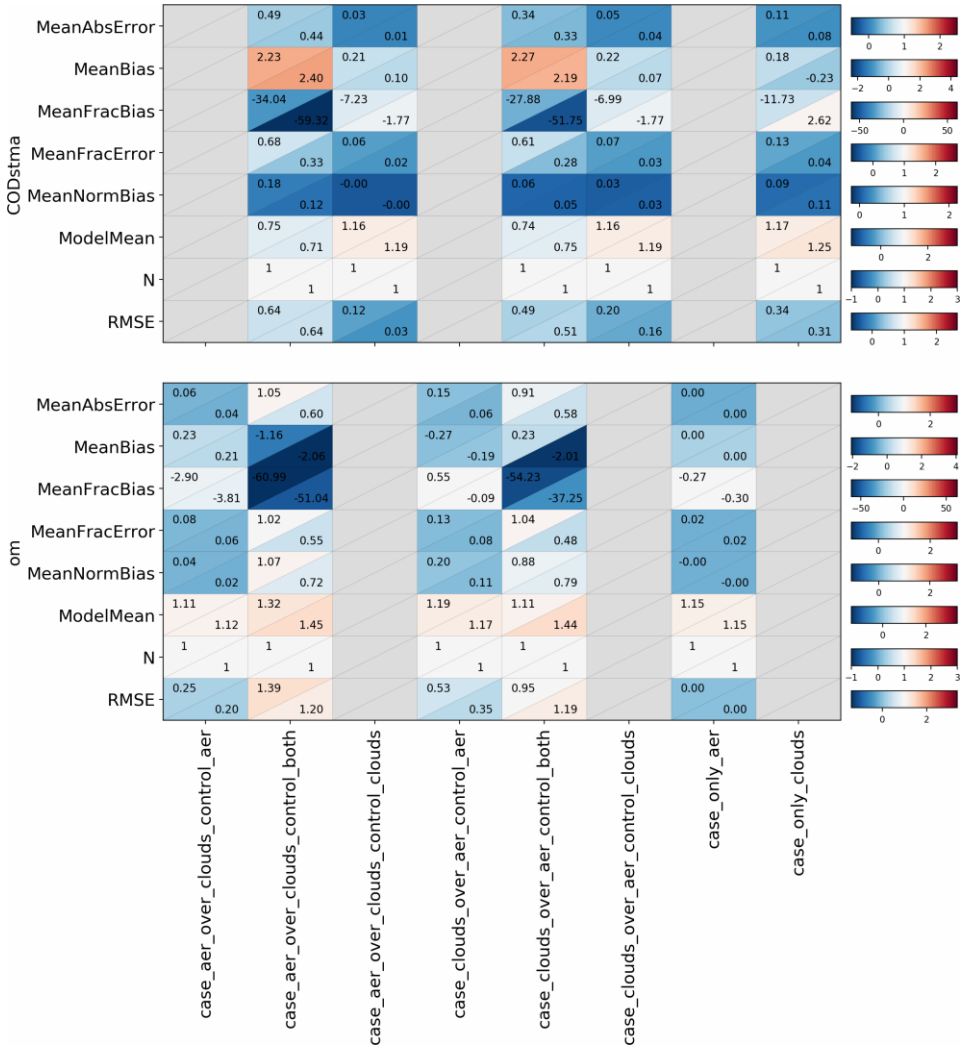

Figure 21: Similar to Figure 15 but using FLOTSAM as radiative transfer model for the true atmosphere and without adding random noise to the simulated observations.

7 Appendix 2: Comparison of RTMs reflectances

The following two figures show a comparison of simulated reflectance between DISORT (yt) and Flotsam (Hxb) simulation for the two simplest cases: only aerosols in Figure 22 and only clouds in Figure 23 .Scatter plots show the same data in different ways. By direct comparison (left), absolute reflectance difference as function of the scattering angle (middle columns) and relative difference, that is, normalised by the reflectance of the DISORT simulations. We show the two simulated channels in rows. The dependency on optical depth (colours) and scattering angle of the difference between the simulations done by these two RTMs is clearly appreciated. Outliers in the left panels are due to numerical issues over affecting DISORT4 original FORTRAN implementation under certain geometrical and optical depth conditions.

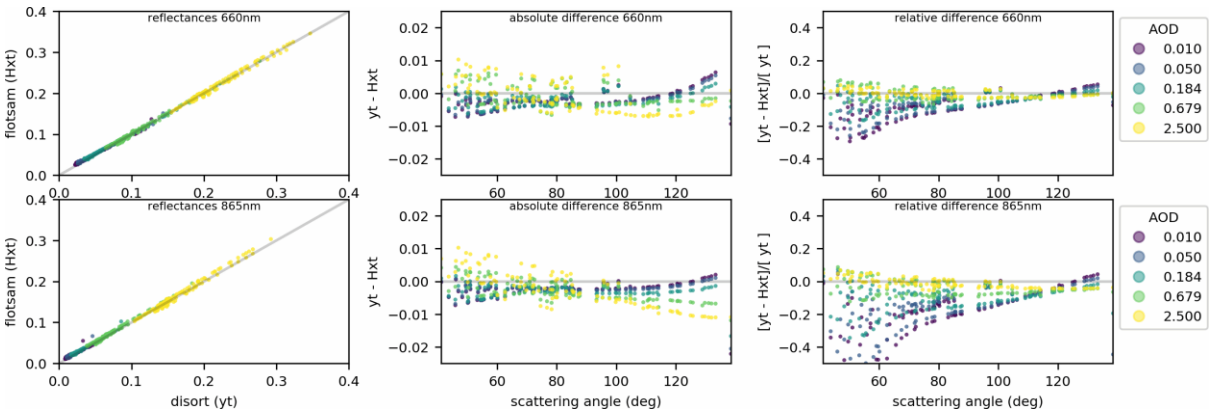

Figure 22:Comparison of simulated reflectances by DISORT and FLOTSAM for the case with only aerosols.

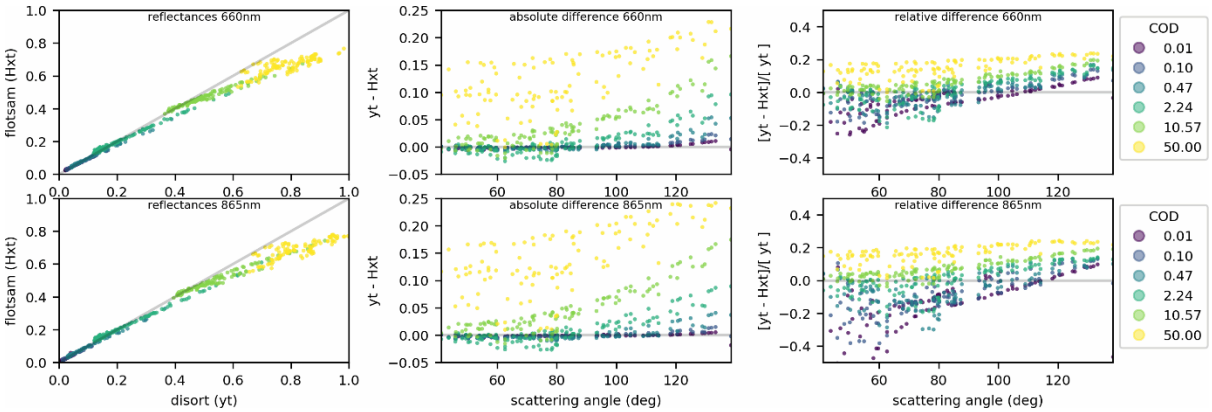

Figure 23:Comparison of simulated reflectances by DISORT and FLOTSAM for the case with only clouds

Document History

Version	Author(s)	Date	Changes
0.0	Jeronimo Escribano	09/05/2024	Initial version
0.2	Jeronimo Escribano	06/06/2024	Addition of comments by E. Emili and new Appendix 2.
0.3	Jeronimo Escribano	12/06/2024	Submitted to internal review
1.1	Jeronimo Escribano	04/07/2024	Revised and issued

Internal Review History

Internal Reviewers	Date	Comments
Philippe CIAIS (CEA) and Marion Schroedter-Homscheidt (DLR)	June 2024	Requested clarification on some points.